Smart Structures and Systems, *Vol. 16, No. 5 (2015) 759-780*
DOI: http://dx.doi.org/10.12989/sss.2015.16.5.759

Unified solutions for piezoelectric bilayer cantilevers and solution modifications

Xianfeng Wang and Zhifei Shi*

School of Civil Engineering, Beijing Jiaotong University, Beijing 100044, P.R. China

(Received Octoebr 31, 2014, Revised February 8, 2015, Accepted February 17, 2015)

Abstract. Based on the theory of piezoelasticity, the static performance of a piezoelectric bilayer cantilever fully covered with electrodes on the upper and lower surfaces is studied. Three models are considered, i.e., the sensor model, the driving displacement model and the blocking force model. By establishing suitable boundary conditions and proposing an appropriate Airy stress function, the exact solutions for piezoelectric bilayer cantilevers are obtained, and the effect of ambient thermal excitation is taken into account. Since the layer thicknesses and material parameters are distinguished in different layers, this paper gives unified solutions for composite piezoelectric bilayer cantilevers including piezoelectric bimorph and piezoelectric heterogeneous bimorph, etc. For some special cases, the simplifications of the present results are compared with other solutions given by other researches based on one-dimensional constitutive equations, and some amendments have been found. The present investigation shows: (1) for a PZT-4 piezoelectric bimorph, the amendments of tip deflections induced by an end shear force, an end moment or an external voltage are about 19.59%, 23.72% and 7.21%, respectively; (2) for a PZT-4-Al piezoelectric heterogeneous bimorph with constant layer thicknesses, the amendments of tip deflections induced by an end shear force, an end moment or an external voltage are 9.85%, 11.78% and 4.07%, respectively, and the amendments of the electrode charges induced by an end shear force or an end moment are both 1.04%; (3) for a PZT-4-Al piezoelectric heterogeneous bimorph with different layer thicknesses, the maximum amendment of tip deflection approaches 23.72%, and the maximum amendment of electrode charge approaches 31.09%. The present solutions can be used to optimize bilayer devices, and the Airy stress function can be used to study other piezoelectric cantilevers including multi-layered piezoelectric cantilevers under corresponding loads.

Keywords: piezoelectric; bimorph; unimorph; sensor; actuator; thermal effect

1. Introduction

Piezoelectric materials are widely used as sensors and actuators in vibration and shape control of flexible structures (Ray and Reddy 2005, Malgaca and Karaguelle 2009, Schoeftner and Irschik 2011). It is usually hoped that a larger displacement, output voltage or blocking force is supplied for most of smart devices. Compared with multilayer structures, a bilayer structure produces a larger displacement as well as output voltage at the same load level (Hauke *et al.* 2000, Xiang and Shi 2009). Therefore, the investigations on the performance and applications of bilayer structures have attracted much attention in recent several decades.

*Corresponding author, Professor, E-mail: zfshi178@bjtu.edu.cn

http://www.techno-press.org/?journal=sss&subpage=8 ISSN: 1738-1584 (Print), 1738-1991 (Online)

Based on one-dimensional piezoelectric constitutive equations, Smits and his co-workers (Smits *et al.* 1991, Smits and Choi 1991, 1993) studied the static performance of both piezoelectric bimorph cantilevers and piezoelectric heterogeneous bimorph cantilevers under loads. Hauke *et al.* (2000) reported experimental results of piezoelectric cantilever actuator and gave a linear regression formula with respect to the number of layers. Based on the theory of piezoelasticity, Shi and his co-workers conducted a series of theoretical solutions for piezoelectric smart devices, including both multi-layered piezoelectric cantilevers and functionally gradient piezoelectric beams (Shi 2002, 2005, Zhang and Shi 2006, Xiang and Shi 2008). Based on the piezoelectric bimorph cantilever models, Erturk and Inman (2009) derived closed-form analytical solutions of both series and parallel bimorph cantilevers. In another paper, Erturk (2011) formulated the problem of vibration-based energy harvesting for civil infrastructure applications.

Exposed to the ambient thermal excitation, the performance of smart devices is seriously affected, which leads to a considerable number of investigations concern about the piezothermoelastic behavior of smart devices. Using the classic shell theory, Tzou and his co-workers derived a generic piezothermoelastic thin shell theory, and discussed the piezothermoelastic characteristics of cylindrical shells, rings, beams and shell laminates (Tzou and Howard 1994, Tzou and Bao 1995). Based on the plate theory, Ashida and Tauchert (1997, 1998) analyzed the stationary and transient response of a finite piezothermoelastic circular disk, in which the inverse problem was also solved to determine the surface temperature according to the electric potential difference between the faces of the disk. In addition, Kapuria *et al.* (2005, 2006) presented third-order unified formulations for both hybrid piezoelectric plates and hybrid piezoelectric functionally graded beams under a thermo-electromechanical load. Based on the theory of piezoelasticity, Shi and his co-workers studied the thermal effects on smart devices including functionally gradient cantilevers, double-layered hollow cylinders and functionally gradient sandwich cantilevers (Chen and Shi 2005a, b, Xiang and Shi 2009).

Though the performance of piezoelectric bimorph cantilevers (Smits *et al.* 1991) and piezoelectric heterogeneous bimorph cantilevers (Smits and Choi 1991, 1993) has been studied based on elementary theories, to the best of our knowledge, the unified solutions for composite piezoelectric bilayer cantilevers based on the theory of piezoelasticity haven't been obtained yet.

In the present study, a bilayer cantilever fully covered with electrodes is investigated based on the theory of piezoelasticity. Since the layer thicknesses and material parameters are distinguished in different layers, the present solutions can be considered as unified solutions for composite piezoelectric bilayer cantilevers. An appropriate Airy stress function is proposed, and the sensor model, driving displacement model and blocking force model are considered. The derived analytical results satisfy all the electromechanical boundary conditions of the cantilever. Moreover, both pyroelectric effect and thermal expansion coefficients (TEC) are taken into account. This work provides a deep understanding and may direct the further applications of composite piezoelectric bilayer cantilevers. The outline of the paper is shown as follows: In Section 2, the two-dimensional constitutive equations of piezoelectric materials are introduced. In Section 3, the unified solutions for composite piezoelectric bilayer cantilevers under three different load cases are obtained. In Section 4, the present solutions are simplified to two different bilayer structures. The simplifications are compared with other investigations based on elementary theories, and some amendments have been found. Numerical analysis and parametric studies are conducted in Section 5. Section 6 concludes the investigation.

2. Basic equations

As shown in Fig. 1, a piezoelectric bilayer cantilever with different layer thickness is considered herein. The upper and lower surfaces of the cantilever are continuously adhered to electrodes, and the lower surface is grounded. The Cartesian coordinate system (x, z) is introduced in the present study to clearly describe the basic equations. While the thermal excitation is taken into account, the temperature field and piezoelastic field are usually decoupled, and the former can be determined separately as a constant field. Therefore, in some investigations (Smits and Choi 1993, Gehring *et al.* 2000, Peng *et al.* 2003), the determination of the temperature field is ignored. In this case, the effect of thermal excitation on the piezoelastic field is considered by adding the temperature increase directly in the piezoelectric constitutive equations (Tzou and Howard 1994, Tzou and Bao 1995). Letting the temperature increase T equals to the absolute temperature minus the stress free temperature, and ε_{ij}, σ_{ij}, D_i as well as E_i denote the components of strain, stress, electric displacement, electric field strength of the piezoelectric media, respectively, the two-dimensional constitutive equations for transversely isotropic piezoelectric material can be expressed as (Tzou and Howard 1994, Tzou and Bao 1995, Xiang and Shi 2009)

$$\begin{cases} \varepsilon_x = S_{11}\sigma_x + S_{13}\sigma_z + d_{31}E_z + \alpha_1 T \\ \varepsilon_z = S_{13}\sigma_x + S_{33}\sigma_z + d_{33}E_z + \alpha_3 T \\ \gamma_{xz} = S_{44}\tau_{xz} + d_{15}E_x \\ D_x = d_{15}\tau_{xz} + e_{11}E_x \\ D_z = d_{31}\sigma_x + d_{33}\sigma_z + e_{33}E_z + p_3 T \end{cases} \tag{1}$$

where S_{ij}, d_{ij}, and e_{ij} are flexible constants, piezoelectric constants and dielectric constants, respectively; α_i and p_3 are TEC and pyroelectric constant, respectively. In this paper, the plane strain hypothesis is introduced. Without consideration of body force and body charge, the equilibrium equations are expressed as

$$\frac{\partial \sigma_x}{\partial x} + \frac{\partial \tau_{xz}}{\partial z} = 0 \quad \frac{\partial \tau_{xz}}{\partial x} + \frac{\partial \sigma_z}{\partial z} = 0 \tag{2}$$

$$\frac{\partial D_x}{\partial x} + \frac{\partial D_z}{\partial z} = 0 \tag{3}$$

The components of strain and electric field strength are related to displacement u, w and electrical potential ϕ by the following equations

$$\varepsilon_x = \frac{\partial u}{\partial x}, \quad \varepsilon_z = \frac{\partial w}{\partial z}, \quad \gamma_{xz} = \frac{\partial u}{\partial z} + \frac{\partial w}{\partial x}, \quad E_x = -\frac{\partial \phi}{\partial x}, \quad E_z = -\frac{\partial \phi}{\partial z} \tag{4}$$

In addition, the compatibility equation expressed by the components of strain is written as

$$\frac{\partial^2 \varepsilon_x}{\partial z^2} + \frac{\partial^2 \varepsilon_z}{\partial x^2} = \frac{\partial^2 \gamma_{xz}}{\partial x \partial z} \tag{5}$$

The substitution of Eq. (1) into Eqs. (5) and (3) results in the following governing equation in terms of the stress (σ_x , σ_z) as well as the electric field strength (E_x , E_z)

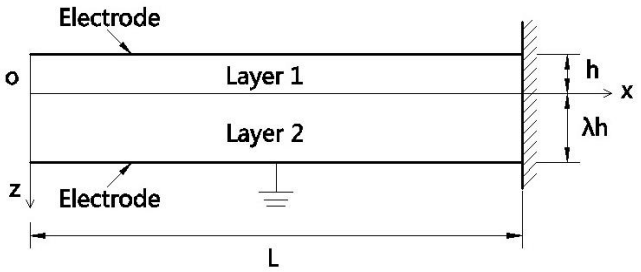

Fig. 1 Schematic of the composite piezoelectric bilayer cantilever

$$\begin{cases} \left[S_{11}\dfrac{\partial^2}{\partial z^2}+\left(S_{13}+\dfrac{S_{44}}{2}\right)\dfrac{\partial^2}{\partial x^2}\right]\sigma_x+\left[S_{33}\dfrac{\partial^2}{\partial x^2}+\left(S_{13}+\dfrac{S_{44}}{2}\right)\dfrac{\partial^2}{\partial z^2}\right]\sigma_z \\ +d_{31}\dfrac{\partial^2 E_z}{\partial z^2}+d_{33}\dfrac{\partial^2 E_z}{\partial x^2}-d_{15}\dfrac{\partial^2 E_x}{\partial x\partial z}=0 \\ d_{31}\dfrac{\partial \sigma_x}{\partial z}+\left(d_{33}-d_{15}\right)\dfrac{\partial \sigma_z}{\partial z}+e_{11}\dfrac{\partial E_x}{\partial x}+e_{33}\dfrac{\partial E_z}{\partial z}=0 \end{cases} \tag{6}$$

Combing with the detailed boundary conditions, the above basic equations will be solved in the following section.

3. Analytical results for three models

Based on Airy stress function method, the exact solutions of piezoelectric bimorph cantilevers subjected to different load cases are obtained in this section. Three models are considered, i.e., the sensor model, the driving displacement model and the blocking force model. The layer thicknesses and material parameters are distinguished in different layers, which results in the unified solutions for composite piezoelectric bilayer cantilevers.

3.1 Airy stress function method

To determine the expressions of the unknown components, the Airy stress function method is used. The stress function φ is introduced to the present study. Hence, the stress components can be expressed as

$$\sigma_x=\frac{\partial^2\varphi}{\partial z^2},\quad \sigma_z=\frac{\partial^2\varphi}{\partial x^2},\quad \tau_{xz}=-\frac{\partial^2\varphi}{\partial x\partial z} \tag{7}$$

In the present study, the mechanical load concentrates on the free end of the bilayer cantilever only. According to the mechanical boundary conditions at the upper and lower surfaces of the beam, the stress component σ_z is assumed to be zero. In this case, the stress function φ is obtained as

$$\varphi(x,z)=a(z)x+b(z) \tag{8}$$

By using Eqs. (7) and (8), the expressions of the stress components can be obtained as

$$\sigma_x(x,z)=a''(z)x+b''(z),\quad \sigma_z(x,z)=0,\quad \tau_{xz}(x,z)=-a'(z) \tag{9}$$

where $a(z)$ and $b(z)$ are prescribed functions. Substituting Eqs. (4) and (9) into Eq. (6) results in the following equations

$$S_{11}a^{(4)}(z)x+S_{11}b^{(4)}(z)-d_{31}\phi_{,zzz}-d_{33}\phi_{,xxz}+d_{15}\phi_{,xxz}=0 \tag{10}$$

$$d_{31}a^{(3)}(z)x+d_{31}b^{(3)}(z)-e_{11}\phi_{,xx}-e_{33}\phi_{,zz}=0 \tag{11}$$

Taking a first derivative of Eq. (11) with respect to the coordinate *z*, the following equation is obtained

$$d_{31}a^{(4)}(z)x+d_{31}b^{(4)}(z)-e_{11}\phi_{,xxz}-e_{33}\phi_{,zzz}=0 \tag{12}$$

By using Eqs. (10) and (12), the third derivative of the electrical potential ($\phi_{,xxz}$, $\phi_{,zzz}$) are obtained, respectively

$$\phi_{,xxz}=A\left[a^{(4)}(z)x+b^{(4)}(z)\right] \tag{13}$$

$$\phi_{,zzz}=B\left[a^{(4)}(z)x+b^{(4)}(z)\right] \tag{14}$$

where

$$A=\frac{e_{33}S_{11}-d_{31}{}^2}{e_{33}d_{33}-e_{11}d_{31}-e_{33}d_{15}},\quad B=\frac{d_{31}-e_{11}A}{e_{33}}$$

According to Eq. (13), the electrical potential ϕ can be expressed as

$$\phi=\frac{A}{6}a^{(3)}(z)x^3+\frac{A}{2}b^{(3)}(z)x^2+g(z)x+r(z)+f(x) \tag{15}$$

where $g(z)$, $r(z)$ as well as $f(x)$ are prescribed functions. According to Eq. (15) and the electric boundary condition $\phi(x,\lambda h)=0$, the prescribed function $f(x)$ is assumed as follows

$$f(x)=f_3x^3+f_2x^2+f_1x \tag{16}$$

Taking a second derivative of the electrical potential ϕ with respect to the coordinate *x* as well as the coordinate *z*, respectively

$$\phi_{,xx}=Aa^{(3)}(z)x+Ab^{(3)}(z)+f''(x) \tag{17}$$

$$\phi_{,zz}=\frac{A}{6}a^{(5)}(z)x^3+\frac{A}{2}b^{(5)}(z)x^2+g''(z)x+r''(z) \tag{18}$$

Substituting Eqs. (17) and (18) into Eq. (11) yields

$$\begin{aligned}&-e_{33}\frac{A}{6}a^{(5)}(z)x^3-e_{33}\frac{A}{2}b^{(5)}(z)x^2+\left[d_{31}a^{(3)}(z)-e_{11}Aa^{(3)}(z)-e_{33}g''(z)-6e_{11}f_3\right]x\\&+d_{31}b^{(3)}(z)-e_{11}Ab^{(3)}(z)-e_{33}r''(z)-2e_{11}f_2=0\end{aligned}\tag{19}$$

Any value of x and z satisfies the equation above, which means

$$\begin{cases}a^{(5)}(z)=0\\b^{(5)}(z)=0\\d_{31}a^{(3)}(z)-e_{11}Aa^{(3)}(z)-e_{33}g''(z)-6e_{11}f_3=0\\d_{31}b^{(3)}(z)-e_{11}Ab^{(3)}(z)-e_{33}r''(z)-2e_{11}f_2=0\end{cases}\tag{20}$$

According to Eqs. (16) and (20), we have

$$\begin{cases}a(z)=a_4z^4+a_3z^3+a_2z^2+a_1z\\b(z)=b_4z^4+b_3z^3+b_2z^2\\g(z)=g_3z^3+g_2z^2+g_1z\\r(z)=r_3z^3+r_2z^2+r_1z+r_0\\f(x)=f_3x^3+f_2x^2+f_1x\end{cases}\tag{21}$$

$$g_3=4Ba_4,\ \ r_3=4Bb_4,\ \ 6Ba_3-2g_2-6\frac{e_{11}}{e_{33}}f_3=0,\ 6Bb_3-2r_2-2\frac{e_{11}}{e_{33}}f_2=0\tag{22}$$

Substituting Eq. (21) into Eqs. (15) and (9) respectively, the electric potential can be expressed in detail as

$$\begin{aligned}\phi(x,z)=&\left(4a_4Az+a_3A+f_3\right)x^3+\left(12b_4Az+3b_3A+f_2\right)x^2\\&+\left(g_3z^3+g_2z^2+g_1z+f_1\right)x+r_3z^3+r_2z^2+r_1z+r_0\end{aligned}\tag{23}$$

The stress components can be expressed in detail as

$$\begin{cases}\sigma_x(x,z)=\left(12a_4z^2+6a_3z+2a_2\right)x+12b_4z^2+6b_3z+2b_2\\\sigma_z(x,z)=0\\\tau_{xz}(x,z)=-4a_4z^3-3a_3z^2-2a_2z-a_1\end{cases}\tag{24}$$

Substituting Eq. (23) into Eq. (4), the electric field strengths are obtained as

$$\begin{cases}E_x(x,z)=-\left(12a_4Az+3a_3A+3f_3\right)x^2-\left(24b_4Az+6b_3A+2f_2\right)x-\left(g_3z^3+g_2z^2+g_1z+f_1\right)\\E_z(x,z)=-4a_4Ax^3-12b_4Ax^2-\left(3g_3z^2+2g_2z+g_1\right)x-\left(3r_3z^2+2r_2z+r_1\right)\end{cases}\tag{25}$$

Further, by using Eqs. (1), (24) and (25), the components of strain and electric displacement can be obtained, respectively

$$\begin{cases}\varepsilon_x(x,z)=-4d_{31}a_4Ax^3-12d_{31}b_4Ax^2+\left[S_{11}\left(12a_4z^2+6a_3z+2a_2\right)-d_{31}\left(3g_3z^2+2g_2z+g_1\right)\right]x\\ \qquad +S_{11}\left(12b_4z^2+6b_3z+2b_2\right)-d_{31}\left(3r_3z^2+2r_2z+r_1\right)+\alpha_1T\\ \varepsilon_z(x,z)=-4d_{33}a_4Ax^3-12d_{33}b_4Ax^2+\left[S_{13}\left(12a_4z^2+6a_3z+2a_2\right)-d_{33}\left(3g_3z^2+2g_2z+g_1\right)\right]x\\ \qquad +S_{13}\left(12b_4z^2+6b_3z+2b_2\right)-d_{33}(3r_3z^2+2r_2z+r_1)+\alpha_3T\\ \gamma_{xz}(x,z)=-d_{15}\left(12a_4Az+3a_3A+3f_3\right)x^2-d_{15}\left(24b_4Az+6b_3A+2f_2\right)x\\ \qquad -d_{15}\left(g_3z^3+g_2z^2+g_1z+f_1\right)-S_{44}\left(4a_4z^3+3a_3z^2+2a_2z+a_1\right)\end{cases} \tag{26}$$

$$\begin{cases}D_x(x,z)=-e_{11}\left(12a_4Az+3a_3A+3f_3\right)x^2-e_{11}\left(24b_4Az+6b_3A+2f_2\right)x\\ \qquad -e_{11}\left(g_3z^3+g_2z^2+g_1z+f_1\right)-d_{15}\left(4a_4z^3+3a_3z^2+2a_2z+a_1\right)\\ D_z(x,z)=-4e_{33}a_4Ax^3-12e_{33}b_4Ax^2+\left[d_{31}\left(12a_4z^2+6a_3z+2a_2\right)-e_{33}\left(3g_3z^2+2g_2z+g_1\right)\right]x\\ \qquad +d_{31}\left(12b_4z^2+6b_3z+2b_2\right)-e_{33}\left(3r_3z^2+2r_2z+r_1\right)+p_3T\end{cases} \tag{27}$$

To determine the components of displacement, the following equations are considered

$$u(x,z)=\int\varepsilon_x dx+u_0(z),\quad w(x,z)=\int\varepsilon_z dz+w_0(x),\quad \gamma_{xz}(x,z)=\frac{\partial u(x,z)}{\partial z}+\frac{\partial w(x,z)}{\partial x} \tag{28}$$

Substituting Eq. (26) into Eq. (28) yields

$$\begin{aligned}u(x,z)=&-d_{31}a_4Ax^4-4d_{31}b_4Ax^3+\left[S_{11}\left(12a_4z^2+6a_3z+2a_2\right)-d_{31}\left(3g_3z^2+2g_2z+g_1\right)\right]\frac{x^2}{2}\\ &+\left[S_{11}\left(12b_4z^2+6b_3z+2b_2\right)-d_{31}\left(3r_3z^2+2r_2z+r_1\right)+\alpha_1T\right]x\\ &-d_{15}\left(\frac{1}{4}g_3z^4+\frac{1}{3}g_2z^3+\frac{1}{2}g_1z^2\right)-S_{44}\left(a_4z^4+a_3z^3+a_2z^2\right)-S_{13}\left(a_4z^4+a_3z^3+a_2z^2\right)\\ &+d_{33}\left(\frac{1}{4}g_3z^4+\frac{1}{3}g_2z^3+\frac{1}{2}g_1z^2\right)-\left(d_{15}f_1+S_{44}a_1+\theta\right)z+u_0\end{aligned} \tag{29}$$

$$\begin{aligned}w(x,z)=&\left[-4d_{33}a_4Az-d_{15}\left(a_3A+f_3\right)-\left(S_{11}a_3-\frac{1}{3}d_{31}g_2\right)\right]x^3\\ &+\left[-12d_{33}b_4Az-d_{15}\left(3b_3A+f_2\right)-\left(3S_{11}b_3-d_{31}r_2\right)\right]x^2\\ &+\left[S_{13}\left(4a_4z^3+3a_3z^2+2a_2z\right)-d_{33}\left(g_3z^3+g_2z^2+g_1z\right)+\theta\right]x\\ &+S_{13}\left(4b_4z^3+3b_3z^2+2b_2z\right)-d_{33}\left(r_3z^3+r_2z^2+r_1z\right)+\alpha_3Tz+w_0\end{aligned} \tag{30}$$

where θ, w_0, u_0 are integration constants.

To distinguish the material parameters as well as the unknown constants in different layers, the subscript *i* is introduced to the present study. Therefore, as a summary, there are 40 unknown constants to be determined

$$\left(a_{4i},a_{3i},a_{2i},a_{1i}\right),\left(b_{4i},b_{3i},b_{2i}\right),\left(g_{3i},g_{2i},g_{1i}\right),\left(r_{3i},r_{2i},r_{1i},r_{0i}\right),\left(f_{3i},f_{2i},f_{1i}\right),\left(u_{0i},w_{0i},\theta_{0i}\right)\ i=1,2$$

With the help of mechanical and electric boundary conditions, all these unknown constants can be determined under different load cases.

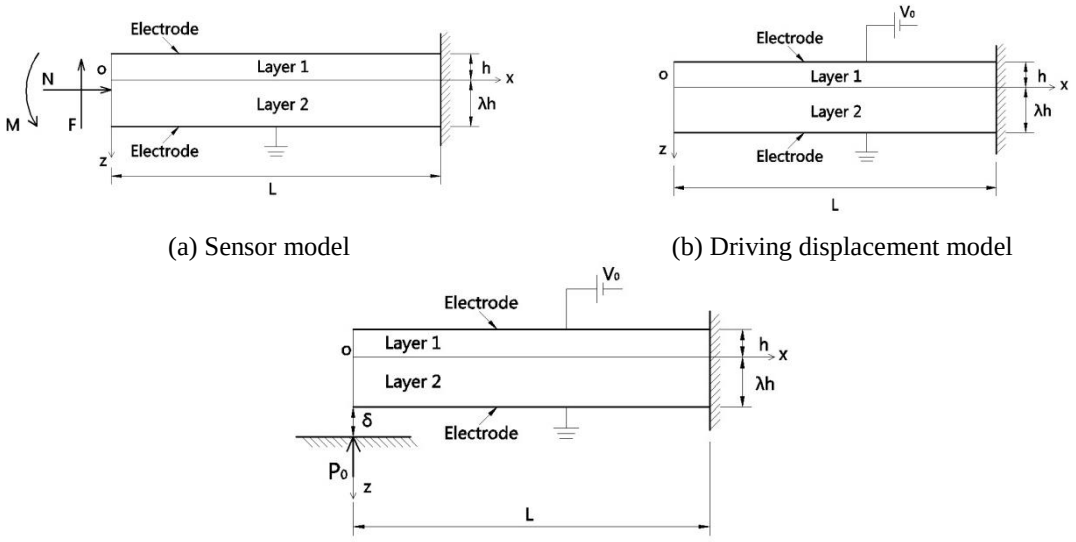

(a) Sensor model

(b) Driving displacement model

(c) Blocking force model

Fig. 2 Three different load cases

3.2 Sensor model

A bilayer cantilever subjected to thermal and mechanical loads is considered. That is, besides being subjected to a steady thermal load T, an end shear force F, an end moment M and an end axial force N are applied at the free end of the cantilever, as shown in Fig. 2(a). That is to say, the following conditions have to be satisfied:

Mechanical boundary conditions

$$\begin{cases} \sigma_{z1}(x,-h)=0 \\ \tau_{xz1}(x,-h)=0 \\ \sigma_{z2}(x,\lambda h)=0 \\ \tau_{xz2}(x,\lambda h)=0 \end{cases} \tag{31}$$

$$\begin{cases} \int_{-h}^{0}\sigma_{x1}(0,z)dz+\int_{0}^{\lambda h}\sigma_{x2}(0,z)dz=-N \\ \int_{-h}^{0}\sigma_{x1}(0,z)zdz+\int_{0}^{\lambda h}\sigma_{x2}(0,z)zdz=-M \\ \int_{-h}^{0}\tau_{xz1}(0,z)dz+\int_{0}^{\lambda h}\tau_{xz2}(0,z)dz=F \end{cases} \tag{32}$$

Electrical boundary conditions

$$\begin{cases} \phi_1(x,-h)=const \\ \phi_2(x,\lambda h)=0 \\ \int_0^L D_{z1}(x,-h)dx=0 \end{cases} \tag{33}$$

Mechanical continuous conditions

$$\begin{cases} \sigma_{z1}(x,0)-\sigma_{z2}(x,0)=0 \\ \tau_{xz1}(x,0)-\tau_{xz2}(x,0)=0 \\ u_1(x,0)-u_2(x,0)=0 \\ w_1(x,0)-w_2(x,0)=0 \end{cases} \tag{34}$$

Electrical continuous conditions

$$\begin{cases} \phi_1(x,0)-\phi_2(x,0)=0 \\ D_{z1}(x,0)-D_{z2}(x,0)=0 \end{cases} \tag{35}$$

For the fixed end, the following conditions have to be satisfied

$$\begin{cases} u_1(L,0)=0 \\ w_1(L,0)=0 \\ \dfrac{\partial w_1}{\partial x}(L,0)=0 \end{cases} \tag{36}$$

Eqs. (31)-(36) combined with Eq. (22) generate 42 equations, of which two are not independent. That is to say, there are 40 independent equations in total. As a composite piezoelectric bilayer cantilever subjected to thermal and mechanical loads as shown in Fig. 2(a), the solutions are listed in Appendix A.

3.3 Driving displacement model

A bilayer cantilever subjected to thermal and electric loads is considered. For the composite piezoelectric bilayer cantilever as shown in Fig. 2(b), besides being subjected to thermal load, an external voltage is applied to the cantilever. Compared with the load case above, some electric boundary conditions have changed, i.e., the electric potential ϕ is equal to V_0 instead of being constant at the upper surface of the cantilever, and the electric displacement boundary condition at the upper surface is not available any more. In this case, the third term in Eq. (33) is supposed to be replaced by the following equation

$$\phi_1(0,-h)=V_0 \tag{37}$$

The mechanical boundary conditions at the free end have changed as well, i.e., Eq. (32) is supposed to be replaced by the following equations

$$\begin{cases} \int_{-h}^{0}\sigma_{x1}(0,z)\,dz+\int_{0}^{\lambda h}\sigma_{x2}(0,z)\,dz=0 \\ \int_{-h}^{0}\sigma_{x1}(0,z)\,z dz+\int_{0}^{\lambda h}\sigma_{x2}(0,z)\,z dz=0 \\ \int_{-h}^{0}\tau_{xz1}(0,z)\,dz+\int_{0}^{\lambda h}\tau_{xz2}(0,z)\,dz=0 \end{cases} \tag{38}$$

With other boundary and continuous conditions unchanged, there are 40 independent equations obtained in total. By using the 40 independent equations, the unknown constants for a composite piezoelectric bilayer cantilever subjected to thermal and electric loads are obtained in Appendix B.

3.4 Blocking force model

A bilayer cantilever subjected to thermal, electric, and mechanical loads simultaneously is considered. Besides being subjected to thermal load, an external voltage is applied to the cantilever as shown in Fig. 2(c). A rigid surface is settled under the cantilever. The initial distance from the lower surface of the cantilever to the rigid surface is δ. With the increase of the applied voltage, the tip deflection of the cantilever at the lower surface increases as well. This model is the same as the driving displacement model while the tip deflection of the cantilever at the lower surface is smaller than δ. However, once the cantilever touches the rigid surface below, a blocking force P_0 is applied to the cantilever. Compared with the driving displacement model, the third term in Eq. (38) is supposed to be replaced by the following equation

$$\int_{-h}^{0} \tau_{xz1}(0,z)\,dz + \int_{0}^{\lambda h} \tau_{xz2}(0,z)\,dz = P_0 \tag{39}$$

By using the 40 independent equations, the 40 unknown constants are obtained in Appendix C. The relation of the applied voltage V_0 and the blocking force P_0 can be simply obtained with the help of the following equation

$$w(0,\lambda h) = \delta \tag{40}$$

where δ is the initial distance from the lower surface of the cantilever to the rigid surface below.

4. Case study and solution modifications

As special cases, two bilayer structures are studied, i.e., a piezoelectric bimorph cantilever and a piezoelectric heterogeneous bimorph cantilever. The simplifications of the present solutions are compared with those obtained by other investigators based on elementary theories, and some amendments have been found.

Case I: piezoelectric bimorph. A piezoelectric bimorph is a piezoelectric bilayer cantilever consists of two piezoelectric layers. Based on one-dimensional constitutive equations, Smits *et al.* (1991) studied the performance of a piezoelectric bimorph with the same layer thickness. For an outward series piezoelectric bimorph, the tip deflections induced by an end shear force F, an end moment M or an external voltage V_0 were given as follows

$$w(0,0) = -\frac{S_{11}L^3F}{2h^3} \tag{41}$$

$$w(0,0) = \frac{3S_{11}L^2M}{4h^3} \tag{42}$$

$$w(0,0) = -\frac{3d_{31}L^2V_0}{8h^2} \tag{43}$$

In the present study, by taking ($-d_{ij1}=d_{ij2}=d_{ij}$, $S_{ij1}=S_{ij2}=S_{ij}$, $e_{ij1}=e_{ij2}=e_{ij}$, $\alpha_{i1}=\alpha_{i2}=\alpha_i$, $p_{3i}=0$, $\lambda=1$), the present solutions can be simplified to the solution of an outward series piezoelectric bimorph, of which layer 2 is polarized in $+z$. By combining Appendix A with Eq. (30), the tip deflection induced by an end shear force F or an end moment M can be given as:

$$w(0,0)=-\frac{S_{11}L^3F}{2h^3}\left[1-\frac{3{d_{31}}^2}{4S_{11}e_{33}}-\frac{{d_{31}}^2}{4\left(4S_{11}e_{33}-3{d_{31}}^2\right)}\right] \tag{44}$$

$$w(0,0)=\frac{3S_{11}L^2M}{4h^3}\left(1-\frac{{d_{31}}^2}{S_{11}e_{33}}\right) \tag{45}$$

By combining Appendix B with Eq. (30), the tip deflection induced by an external voltage V_0 can be given as

$$w(0,0)=-\frac{3d_{31}L^2V_0}{8h^2}\left[1-\frac{{d_{31}}^2}{\left(4S_{11}e_{33}-3{d_{31}}^2\right)}\right] \tag{46}$$

The extra terms in Eqs. (44)-(46) are amendments for Eqs. (41)-(43). For a PZT-4 bimorph, the tip deflections induced by an end shear force, an end moment, or an external voltage are smaller than Smits' solutions (Smits *et al.* 1991). The amendments are 19.59%, 23.72% and 7.21%, respectively. The material parameters of PZT-4 are listed in Table 1 (Xiang and Shi 2009). As for the expressions of electrode charges induced by an end shear force or an end moment, the present results agree with Smits' solutions (Smits *et al.* 1991).

Case II: piezoelectric heterogeneous bimorph. A piezoelectric heterogeneous bimorph is a piezoelectric bilayer cantilever made up by a piezoelectric layer joined over its entire length to a non-piezoelectric layer. The non-piezoelectric layer is often made from metal. A piezoelectric heterogeneous bimorph is also called a piezoelectric unimorph. Regardless of pyroelectric effect and TEC, Smits and Choi (1991) studied the static performance of a piezoelectric heterogeneous bimorph. In their solutions, the layer thicknesses are distinguished in different layers. To make the theoretical modifications simple, we assume the two layers are as thick as each other. In this case, Smits and Choi (1991) gave the tip deflections of a piezoelectric heterogeneous bimorph induced by an end shear force F, an end moment M, or an external voltage V_0, respectively, as follows

$$w(0,0)=-\frac{4S_{111}S_{112}\left(S_{111}+S_{112}\right)L^3F}{\left({S_{111}}^2+14S_{111}S_{112}+{S_{112}}^2\right)h^3} \tag{47}$$

$$w(0,0)=\frac{6S_{111}S_{112}\left(S_{111}+S_{112}\right)L^2\,\mathrm{M}}{\left({S_{111}}^2+14S_{111}S_{112}+{S_{112}}^2\right)h^3} \tag{48}$$

$$w(0,0)=\frac{6S_{111}S_{112}d_{31}L^2V_0}{\left({S_{111}}^2+14S_{111}S_{112}+{S_{112}}^2\right)h^2} \tag{49}$$

Smits and Choi (1991) also gave the electrode charges induced by an end shear force F or an end moment M, as follows

$$Q=\frac{6S_{111}S_{112}d_{31}L^2F}{\left({S_{111}}^2+14S_{111}S_{112}+{S_{112}}^2\right)h^2} \tag{50}$$

$$Q=-\frac{12S_{111}S_{112}d_{31}LM}{\left({S_{111}}^2+14S_{111}S_{112}+{S_{112}}^2\right)h^2} \tag{51}$$

In the present paper, by taking (d_{ij2}=0, p_{3i}=0, T=0 and λ=1), the present solutions can be

simplified to the solution of a piezoelectric heterogeneous bimorph with constant layer thicknesses. By taking ($e_{ij2} \to \infty$), the lower layer can be considered as metal. By combining Appendix A and Appendix B with Eq. (30), the tip deflections induced by an end shear force F, an end moment M or an external voltage V_0 can be given as

$$w(0,0) = -\frac{4S_{111}S_{112}\left(S_{111}+S_{112}\right)L^3F}{\left(S_{111}^{\ 2}+14S_{111}S_{112}+S_{112}^{\ 2}\right)h^3}\left(1-H_1\right) \tag{52}$$

$$w(0,0) = \frac{6S_{111}S_{112}\left(S_{111}+S_{112}\right)L^2\,\mathrm{M}}{\left(S_{111}^{\ 2}+14S_{111}S_{112}+S_{112}^{\ 2}\right)h^3}\left(1-H_2\right) \tag{53}$$

$$w(0,0) = \frac{6S_{111}S_{112}d_{311}L^2V_0}{\left(S_{111}^{\ 2}+14S_{111}S_{112}+S_{112}^{\ 2}\right)h^2}\left(1-H_3\right) \tag{54}$$

The output voltage (V) and electrode charge (Q) have the following relation

$$Q = \frac{e_{33}VA_r}{h} \tag{55}$$

where A_r is the area of one surface electrode. Using Eqs. (23) and Appendix A to determine the output voltage (V), the electrode charges induced by an end shear force or an end moment can be given as

$$Q = \frac{6S_{111}S_{112}d_{31}L^2F}{\left(S_{111}^{\ 2}+14S_{111}S_{112}+S_{112}^{\ 2}\right)h^2}\left(1-H_4\right) \tag{56}$$

$$Q = -\frac{12S_{111}S_{112}d_{31}LM}{\left(S_{111}^{\ 2}+14S_{111}S_{112}+S_{112}^{\ 2}\right)h^2}\left(1-H_4\right) \tag{57}$$

The influence of axial force N is ignored in Smits' solution. It should be point out that for a heterogeneous bimorph, the axial force N also contributes to the tip deflections and the electrode charges, which can be proved from the present solutions by taking (M=0, F=0).

The terms from H_1 to H_4 are amendments for Eqs. (47)-(51). The expressions of H_1-H_4 are presented in Appendix D. For a piezoelectric heterogeneous bimorph polarized in –z made from PZT-4 and aluminum, the present results are smaller than Smits' solution. The amendments for tip deflections induced by an end shear force, an end moment or an external voltage are 9.85%, 11.78% and 4.07%, respectively; the amendments for electrode charges induced by an end shear force or an end moment are both 1.04%. The material parameters of aluminum for plane strain problem are transferred from typical aluminum parameters (Peng *et al.* 2003). The material parameters of PZT-4 and aluminum are listed in Table 1. Since the piezoelectric layer is polarized in –z, a negative sign should be given to the piezoelectric constants.

In practical applications, the layer thicknesses of a piezoelectric heterogeneous bimorph can be different. Due to the complexity of the problem, the dependences of modifications on thickness ratio are presented numerically in the following discussions. A fixed total thickness is taken into account. A PZT-4-Al piezoelectric heterogeneous bimorph is adopted, of which layer 1 is made from PZT-4 and polarized in –z. It should be pointed out that the percentage modifications

presented in the following discussions are related only to the material parameters and the thickness ratio.

In the following discussion, the total thickness H=2 mm, the length of the cantilever L=100 mm, and the layer 1-to-total thickness ratio $1/(1+\lambda)$ is set as η. By taking ($h=\eta H$ and $\lambda=1/\eta-1$), the solutions presented in the Appendixes A-C can be transferred to the solutions of a piezoelectric heterogeneous bimorph with fixed total thickness H and layer 1-to-total thickness ratio η. The layer 1-to-total thickness ratio ranges from 0 to 1. The differences between the present result and Smits' solution are highlight in Figs. 3 and 4 since the total thickness of the cantilever is fixed, which leads to a terminate stiffness of the cantilever. In addition, comprehensive percentage modifications are obtained since the piezoelectric thickness ratio varies from a complete non-piezoelectric cantilever to a complete piezoelectric cantilever.

The electrode charge modifications for a piezoelectric unimorph cantilever subjected to an end shear force F or an end moment M are plotted in Figs. 3(a) and 3(b), respectively. We can learn from the theoretical results that these two load cases have the same percentage electrode charge modifications. With the layer 1-to-total thickness ratio η increasing from 0 to 1, the electrode charge modifications monotonically vary from 31.09% to -23.72%.

The tip deflection modifications for a piezoelectric unimorph cantilever subjected to an end shear force F, an end moment M or an external voltage V_0 are plotted in Figs. 4(a)-4(c), respectively. With the layer 1-to-total thickness ratio η increasing from 0 to 1, the tip deflection modifications of these three load cases monotonically vary from 0 to -23.72%.

As a summary of the percentage modifications presented in Figs. 3 and 4, the maximum electrode charge amendment is obtained as 31.09% at η=0 for both end shear force or end moment excitation, and the maximum tip deflection amendment is obtained as -23.72% at η=1 for end shear force, end moment or external voltage excitation.

5. Numerical results

In this section, some parametric study will be conducted to highlight the influence of temperature change and material composition on the static behavior of composite piezoelectric bilayer cantilevers by using the unified solutions obtained in Section 3.

Table1 Material parameters of PZT-4 and aluminum for plain strain problem

Material	Flexible constant (10^{-12}m^{2}N^{-1})	Piezoelectric constant (10^{-12}CN^{-1})	Dielectric constant (10^{-12}C^{2}m^{-2}N^{-1})	TEC (10^{-6}K^{-1})	Pyroelectric constant (10^{-5}Cm^{-2}K^{-1})
PZT-4	$S_{11}=10.97$ $S_{13}=-7.06$ $S_{33}=13.21$ $S_{44}=39.00$	$d_{31}=-163.5$ $d_{33}=235.9$ $d_{15}=469.0$	$e_{11}=1475\times8.85$ $e_{33}=1161\times8.85$	$\alpha_1=1.97$ $\alpha_3=2.62$	$p_3=5.48$
Al	$S_{11}=13.00$ $S_{13}=-5.57$ $S_{33}=13.00$ $S_{44}=37.14$	0	∞	$\alpha_1=30.16$ $\alpha_3=30.16$	0

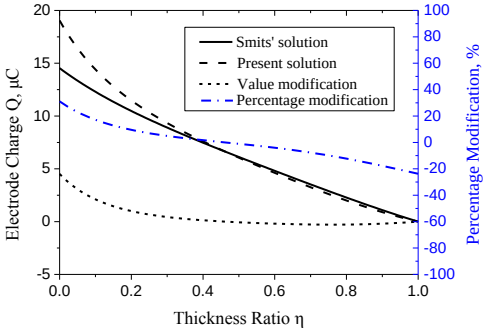

(a) Subjected to an end shear force F=10 N

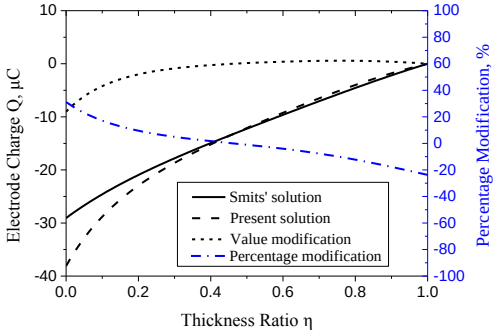

(b) Subjected to an end moment M=1 N·m

Fig. 3 Electrode charge modifications for fixed total thickness H=2 mm

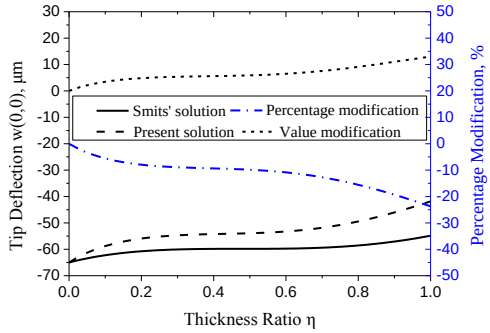

(a) Subjected to an end shear force F=10 N

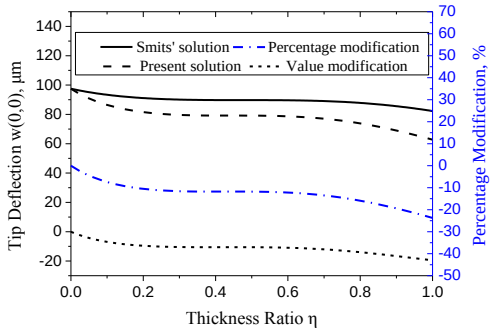

(a) Subjected to an end shear force F=10 N

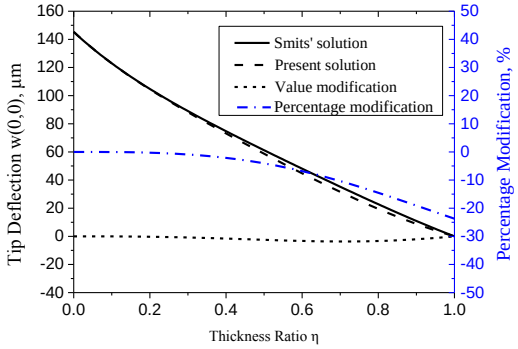

(c) Subjected to an external voltage V_0=100 V

Fig. 4 Tip deflection modifications for fixed total thickness H=2 mm

A PZT-4 piezoelectric bimorph cantilever and a PZT-4-Al piezoelectric heterogeneous bimorph cantilever are considered. In this section, the piezoelectric heterogeneous bimorph is renamed as unimorph. These two kinds of cantilevers are assumed to have the same dimensions L=100 mm, h=1 mm, λ=1. The lower surfaces of these two cantilevers are grounded. The material parameters are listed in Table 1.

For the sensor model, the electric potential distribution at any cross section of a PZT-4 bimorph cantilever subjected to thermal excitation only is plotted in Fig. 5. Four polarization cases are considered as listed in Table 2. Obviously, the potential of the beam on the upper surface for Case 1 and Case 4 is greater than that for Case 2 and Case 3. The electric potential distribution of a PZT-4-Al unimorph cantilever subjected to thermal excitation only is plotted in Fig. 6. The upper layer is polarized in -z. As we can see, the electric potential of the aluminum layer maintains 0, which complies with the characteristic of ideal conductor placed in static electric field. In Fig. 6, the electric potential induced by thermal expansion effect and pyroelectric effect is plotted separately. We can learn from the summation of these two effects that the potential on the upper surface of the beam is nearly 0. This is because the TEC of aluminum is larger than that of PZT-4. With the increasing of temperature, the TEC difference between aluminum and PZT-4 causes tension in PZT-4 layer. Since the PZT-4 layer is polarized in -z, the electric potential on the upper surface of the beam induced by tension is negative, which balances the positive electric potential induced by pyroelectric effect. If the PZT-4 layer were polarized in +z, the electric potential on the upper surface induced by these two effects offsets each other as well. This phenomenon suggests that a unimorph device with suitable dimensions could eliminate the effect of thermal noise when used to transform external forces into electric signals. On the other hand, if the TEC of the non-piezoelectric layer is smaller than that of PZT-4, the electric potential induced by thermal expansion effect would be added to that induced by pyroelectric effect producing a stronger electric signal. An efficient thermal sensor could be developed in this way.

For the driving displacement model, Fig. 7 shows the electric field strength distribution of both bimorph and unimorph cantilevers. It is found that the electric field strength is not constant in piezoelectric layers, and the slope of a unimorph cantilever is the same as that of a bimorph cantilever while the temperature increase T=0. However, the average of electric field strength is 100 kV/m in unimorph cantilever and 50 kV/m in bimorph cantilever, which is equal to the constant electric field (V_0/h) assumed in other works (Smits *et al.* 1991, Smits and Choi 1991).

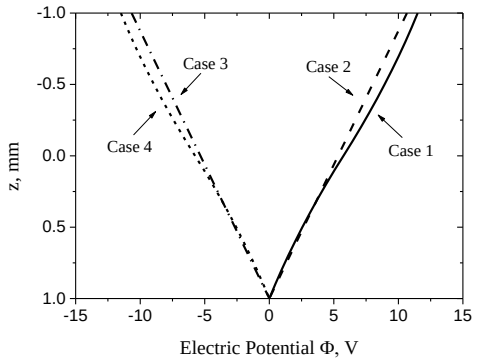

Fig. 5 Electric potential distribution of a piezoelectric bimorph cantilever. T=1 K

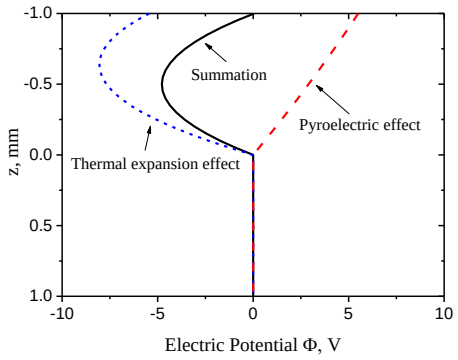

Fig. 6 Electric potential distribution of a piezoelectric unimorph cantilever. T=1 K

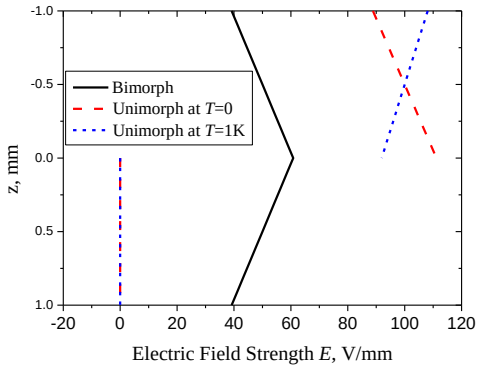

Fig. 7 Electric field strength distribution of both bimorph and unimorph cantilevers for driving displacement model. V_0=100 V

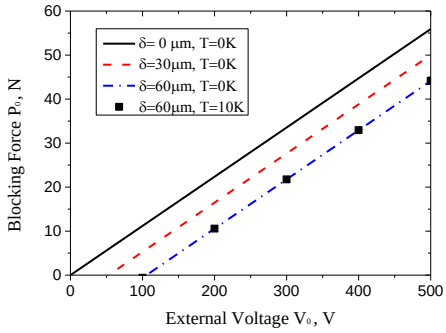

Fig. 8 Bimorph based blocking force induced by an external voltage

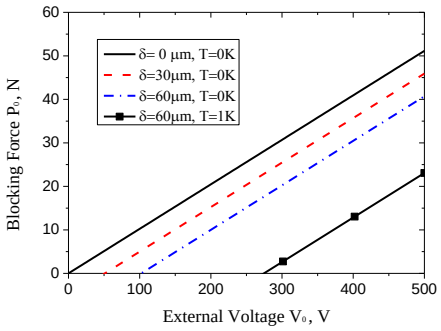

Fig. 9 Unimorph based blocking force induced by an external voltage

Table 2 Cases of polarization

Layer	Case 1	Case 2	Case 3	Case 4
1	In -z direction (↑)	In -z direction (↑)	In +z direction (↓)	In +z direction (↓)
2	In +z direction (↓)	In -z direction (↑)	In +z direction(↓)	In -z direction (↑)

With the temperature increase T=1K, the electric field strength of a bimorph cantilever is unaffected while that of a unimorph is seriously affected. But the average of electric field strength in the piezoelectric layer of a unimorph cantilever maintains 100 kV/m.

For the blocking force model, Figs. 8 and 9 show the relationship between blocking force P_0 and external voltage V_0 for a bimorph cantilever and a unimorph cantilever, respectively. Obviously, the blocking force created by a unimorph cantilever is seriously affected by temperature increase while the blocking force created by a bimorph cantilever is insensitive to temperature change.

6. Conclusions

Based on the theory of piezoelasticity, the static performance of a piezoelectric bilayer cantilever fully covered with electrodes on the upper and lower surfaces is investigated. Three models are considered, i.e., the sensor model, the driving displacement model and the blocking force model. Since the layer thicknesses and material parameters are distinguished in different layers, the present solutions can be considered as unified solutions for composite piezoelectric bilayer cantilevers. The simplifications of the present results are compared with that obtained based on one-dimensional constitutive equations, and some amendments have been found. It should be pointed out that all the percentage modifications mentioned in the present paper are related only to the material parameters and the thickness ratio of the bilayer cantilevers. Some conclusions can be drawn as follows:

- For a piezoelectric bimorph cantilever, the amendments of tip deflections induced by an end

shear force, an end moment or an external voltage are 19.59%, 23.72% and 7.21%, respectively.

- For a piezoelectric unimorph cantilever with constant layer thicknesses, the amendments of tip deflections induced by an end shear force, an end moment or an external voltage are 9.85%, 11.78% and 4.07%, respectively; the amendments of electrode charges induced by an end shear force or an end moment are both 1.04%.
- For a piezoelectric unimorph cantilever with different layer thicknesses, the dependences of modifications on thickness ratio are numerically presented in Figs. 3 and 4. When the layer 1-to-total thickness ratio η approaches 0, the maximum electrode charge amendment is obtained as 31.09%; when the layer 1-to-total thickness ratio η approaches 1, the maximum tip deflection amendment is obtained as 23.72%.

The present solutions can be used to optimize bilayer devices. And the Airy stress function can be used to study other piezoelectric cantilevers including multi-layered piezoelectric cantilevers under corresponding loads.

Acknowledgements

This work is supported by the National Natural Science Foundation of China (51472022).

References

Ashida, F. and Tauchert, T.R. (1997), "Temperature determination for a contacting body based on an inverse piezothermoelastic problem", *Int. J. Solids Struct.*, **34**(20), 2549-2561.

Ashida, F. and Tauchert, T.R. (1998), "Transient response of a piezothermoelastic circular disk under axisymmetric heating", *Acta Mech.*, **128**(1-2), 1-14.

Chen, Y. and Shi, Z.F. (2005a), "Double-layered piezothermoelastic hollow cylinder under thermal loading", *Key Eng Mater.*, **302**, 684-692.

Chen, Y. and Shi, Z.F. (2005b), "Exact solutions of functionally gradient piezothermoelastic cantilevers and parameter identification", *J. Intel. Mat. Syst. Str.*, **16**(6), 531-539.

Erturk, A. (2011), "Piezoelectric energy harvesting for civil infrastructure system applications: Moving loads and surface strain fluctuations", *J. Intel. Mat. Syst. Str.*, **22**(17), 1959-1973.

Erturk, A. and Inman, D.J. (2009), "An experimentally validated bimorph cantilever model for piezoelectric energy harvesting from base excitations", *Smart Mater Struct.*, **18**(2), 25009.

Gehring, G.A., Cooke, M.D., Gregory, I.S., Karl, W.J. and Watts, R. (2000), "Cantilever unified theory and optimization for sensors and actuators", *Smart Mater Struct.*, **9**(6), 918-931.

Hauke, T., Kouvatov, A., Steinhausen, R., Seifert, W., Beige, H. and Theo, H. *et al.* (2000), "Bending behavior of functionally gradient materials", *Ferroelectrics*, **238**(1), 195-202.

Kapuria, S. and Achary, G. (2005), "A coupled consistent third-order theory for hybrid piezoelectric plates", *Compos Struct.*, **70**(1), 120-133.

Kapuria, S., Bhattacharyya, M. and Kumar, A.N. (2006), "Assessment of coupled 1D models for hybrid piezoelectric layered functionally graded beams", *Compos Struct.*, **72**(4), 455-468.

Malgaca, L. and Karaguelle, H. (2009), "Simulation and experimental analysis of active vibration control of smart beams under harmonic excitation", *Smart Struct. Syst.*, **5**(1), 55-68.

Peng, W.Y., Xiao, Z.X. and Farmer, K.R. (2003), "Optimization of thermally actuated bimorph cantilevers for maximum deflection", *Nanotechnology Conference and Trade Show (Nanotech 2003)*, San Francisco, USA, February.

Ray, M.C. and Reddy, J.N. (2005), "Active control of laminated cylindrical shells using piezoelectric fiber

reinforced composites", *Compos Sci. Technol.*, **65**(7-8), 1226-1236.
Schoeftner, J. and Irschik, H. (2011), "Passive shape control of force-induced harmonic lateral vibrations for laminated piezoelastic Bernoulli-Euler beams-theory and practical relevance", *Smart Struct. Syst.*, **7**(5), 417-432.
Shi, Z.F. (2002), "General solution of a density functionally gradient piezoelectric cantilever and its applications", *Smart Mater Struct.*, **11**(1), 122-129.
Shi, Z.F. (2005), "Bending behavior of piezoelectric curved actuator", *Smart Mater Struct.*, **14**(4), 835-842.
Smits, J.G. and Choi, W. (1991), "The constituent equations of piezoelectric heterogeneous bimorphs", *IEEE T. Ultrason Ferr.*, **38**(3), 256-270.
Smits, J.G. and Choi, W. (1993), "Equations of state including the thermal domain of piezoelectric and pyroelectric heterogeneous bimorphs", *Ferroelectrics*, **141**(1), 271-276.
Smits, J.G., Dalke, S.I. and Cooney, T.K. (1991), "The constituent equations of piezoelectric bimorphs", *Sensor Actuat. A-Phys.*, **28**(1), 41-61.
Tzou, H.S. and Bao, Y. (1995), "A theory on anisotropic piezothermoelastic shell laminates with sensor/actuator applications", *J. Sound Vib.*, **184**(3), 453-473.
Tzou, H.S. and Howard, R.V. (1994), "A piezothermoelastic thin shell theory applied to active structures", *J. Vib. Acoust.*, **116**(3), 295-302.
Xiang, H.J. and Shi, Z.F. (2008), "Static analysis for multi-layered piezoelectric cantilevers", *Int. J. Solids Struct.*, **45**(1), 113-128.
Xiang, H.J. and Shi, Z.F. (2009), "Static analysis for functionally graded piezoelectric actuators or sensors under a combined electro-thermal load", *Eur. J .Mech. A-Solid.*, **28**(2), 338-346.
Zhang, T.T. and Shi, Z.F. (2006), "Two-dimensional exact analysis for piezoelectric curved actuators", *J Micromech. Microeng.*, **16**(3), 640-647.

BS

Appendix A

For the piezoelectric layer polarized in -z, a negative sign should be given to the piezoelectric and pyroelectric constants. For a composite piezoelectric bilayer cantilever subjected to thermal and mechanical loads, the 40 unknown constants are determined as (i=1, 2):

$$a_{4i}=b_{4i}=g_{3i}=r_{3i}=0$$

$$\begin{cases} a_{31}=\dfrac{2\left(\lambda J_1+J_2\right)M_2 e_{331}e_{332}F}{h^3 Q_a} \\ a_{32}=\dfrac{M_1}{M_2}a_{31} \end{cases} \quad \begin{cases} a_{21}=\dfrac{(4+3\lambda)h}{2(1+\lambda)}a_{31}+\dfrac{\lambda^3 h}{2(1+\lambda)}a_{32}-\dfrac{F}{(1+\lambda)h^2} \\ a_{22}=-\dfrac{h}{2\lambda(1+\lambda)}a_{31}-\dfrac{\lambda(3+4\lambda)h}{2(1+\lambda)}a_{32}+\dfrac{F}{\lambda(1+\lambda)h^2} \end{cases}$$

$$\begin{cases} g_{2i}=\dfrac{3d_{31i}}{e_{33i}}a_{3i} \\ g_{11}=\dfrac{2d_{311}d_{312}-2S_{111}e_{332}}{d_{312}e_{331}-d_{311}e_{332}}a_{21}+\dfrac{2S_{112}e_{332}-2{d_{312}}^2}{d_{312}e_{331}-d_{311}e_{332}}a_{22} \\ g_{12}=\dfrac{2{d_{311}}^2-2S_{111}e_{331}}{d_{312}e_{331}-d_{311}e_{332}}a_{21}+\dfrac{2S_{112}e_{331}-2d_{311}d_{312}}{d_{312}e_{331}-d_{311}e_{332}}a_{22} \end{cases} \quad \begin{cases} b_{21}=\dfrac{(4+3\lambda)h}{2(1+\lambda)}b_{31}+\dfrac{\lambda^3 h}{2(1+\lambda)}b_{32}-\dfrac{(\lambda hN-2M)}{2(1+\lambda)h^2} \\ b_{22}=-\dfrac{h}{2\lambda(1+\lambda)}b_{31}-\dfrac{\lambda(3+4\lambda)h}{2(1+\lambda)}b_{32}-\dfrac{(hN+2M)}{2\lambda(1+\lambda)h^2} \end{cases}$$

$$\begin{cases} b_{31}=-\dfrac{\left[\begin{array}{l}(2M+hN)\left({d_{312}}^2e_{331}-e_{331}e_{332}S_{112}\right) \\ +\left(2\lambda M-\lambda^2 hN\right)\left({d_{311}}^2e_{332}-e_{331}e_{332}S_{111}\right)\end{array}\right]M_2}{h^3Q_b} \\ \qquad -\dfrac{\lambda(1+\lambda)\left({d_{311}}^2e_{332}-e_{331}e_{332}S_{111}\right)LM_2}{hQ_b}a_{21} \\ \qquad +\dfrac{\lambda(1+\lambda)\left({d_{312}}^2e_{331}-e_{331}e_{332}S_{112}\right)LM_2}{hQ_b}a_{22} \\ \qquad -\dfrac{\lambda(1+\lambda)\left[\begin{array}{l}e_{331}e_{332}(\alpha_{12}-\alpha_{11}) \\ +p_{31}\left(d_{311}e_{332}-d_{312}e_{331}\right)\end{array}\right]TM_2}{hQ_b} \\ b_{32}=\dfrac{M_1}{M_2}b_{31} \end{cases} \quad \begin{cases} r_{2i}=\dfrac{3d_{31i}}{e_{33i}}b_{3i} \\ r_{11}=\dfrac{2d_{311}d_{312}-2S_{111}e_{332}}{d_{312}e_{331}-d_{311}e_{332}}b_{21}+\dfrac{2S_{112}e_{332}-2{d_{312}}^2}{d_{312}e_{331}-d_{311}e_{332}}b_{22} \\ \qquad +\dfrac{e_{332}(\alpha_{12}-\alpha_{11})T}{d_{312}e_{331}-d_{311}e_{332}} \\ r_{12}=\dfrac{2{d_{311}}^2-2S_{111}e_{331}}{d_{312}e_{331}-d_{311}e_{332}}b_{21}+\dfrac{2S_{112}e_{331}-2d_{311}d_{312}}{d_{312}e_{331}-d_{311}e_{332}}b_{22} \\ \qquad +\dfrac{e_{331}(\alpha_{12}-\alpha_{11})T}{d_{312}e_{331}-d_{311}e_{332}} \\ r_{01}=r_{02}=-r_{22}\lambda^2h^2-r_{12}\lambda h \end{cases}$$

$$\begin{cases} \theta_1=\theta_2=3L^2\left(S_{111}a_{31}-\dfrac{1}{3}d_{311}g_{21}\right) \\ \qquad +2L\left(3S_{111}b_{31}-d_{311}r_{21}\right) \\ u_{01}=u_{02}=-\dfrac{L^2}{2}\left(2S_{111}a_{21}-d_{311}g_{11}\right) \\ \qquad -L\left(2S_{111}b_{21}-d_{311}r_{11}+\alpha_{11}T\right) \\ w_{01}=w_{02}=-2L^3\left(S_{111}a_{31}-\dfrac{1}{3}d_{311}g_{21}\right) \\ \qquad -L^2\left(3S_{111}b_{31}-d_{311}r_{21}\right) \end{cases} \quad \begin{cases} J_i=\dfrac{2d_{31i}\left(\lambda d_{311}+d_{312}\right)-2S_{11i}\left(\lambda e_{331}+e_{332}\right)}{d_{312}e_{331}-d_{311}e_{332}} \\ M_i=S_{11i}-\dfrac{{d_{31i}}^2}{e_{33i}} \\ A_i=\dfrac{e_{33i}S_{11i}-{d_{31i}}^2}{e_{33i}d_{33i}-e_{11i}d_{31i}-e_{33i}d_{15i}} \end{cases}$$

$$\begin{cases} Q_a = e_{331}e_{332}\left(\lambda^4 J_1 M_1 + 4\lambda^3 J_2 M_1 + 3\lambda^2 J_2 M_1 + 3\lambda^2 J_1 M_2 + 4\lambda J_1 M_2 + J_2 M_2\right) \\ \quad + 6\lambda(1+\lambda)\left(\lambda^2 M_1 \mathrm{d}_{312} e_{331} - M_2 \mathrm{d}_{311} e_{332}\right) \\ Q_b = \left(\lambda^4 M_1 + 3\lambda^2 M_2 + 4\lambda M_2\right)\left(d_{311}{}^2 e_{332} - e_{331} e_{332} S_{111}\right) \\ \quad + \left(4\lambda^3 M_1 + 3\lambda^2 M_1 + M_2\right)\left(d_{312}{}^2 e_{331} - e_{331} e_{332} S_{112}\right) \end{cases} \quad \begin{cases} f_{3i} = -a_{3i} A_i \\ f_{2i} = -3b_{3i} A_i \\ f_{11} = f_{12} = -g_{21} h^2 + g_{11} h \end{cases}$$

Appendix B

For a composite piezoelectric bilayer cantilever subjected to thermal and electric loads, the 40 unknown constants are determined as (i=1, 2):

$$a_{4i} = a_{3i} = a_{2i} = a_{1i} = g_{3i} = g_{2i} = g_{1i} = b_{4i} = r_{3i} = f_{3i} = f_{1i} = 0$$

$$\begin{cases} b_{31} = -\dfrac{2\lambda(1+\lambda)e_{331}e_{332}M_2 V_0}{h^2 Q_a} \\ \quad + \dfrac{2\lambda(1+\lambda)(\lambda e_{331} + e_{332})e_{331}e_{332}M_2 T(\alpha_{12} - \alpha_{11})}{h(d_{311}e_{332} - d_{312}e_{331})Q_a} \\ b_{32} = \dfrac{M_1}{M_2} b_{31} \end{cases} \quad \begin{cases} b_{21} = \dfrac{(4+3\lambda)h}{2(1+\lambda)} b_{31} + \dfrac{\lambda^3 h}{2(1+\lambda)} b_{32} \\ b_{22} = -\dfrac{h}{2\lambda(1+\lambda)} b_{31} - \dfrac{\lambda(3+4\lambda)h}{2(1+\lambda)} b_{32} \end{cases}$$

The expressions of $r_{2i}, r_{1i}, r_{0i}, f_{3i}, f_{2i}, f_{1i}, \theta_i, u_{0i}, w_{0i}, J_i, M_i, A_i, Q_a$ refer to Appendix A.

Appendix C

For a composite piezoelectric bilayer cantilever subjected to thermal, mechanical and electric loads, the 40 unknown constants are determined as (i=1, 2):

$$a_{4i} = b_{4i} = g_{3i} = r_{3i} = 0$$

$$\begin{cases} a_{31} = \dfrac{2(\lambda J_1 + J_2)M_2 e_{331} e_{332} P_0}{h^3 Q_a} \\ a_{32} = \dfrac{M_1}{M_2} a_{31} \end{cases} \quad \begin{cases} a_{21} = \dfrac{(4+3\lambda)h}{2(1+\lambda)} a_{31} + \dfrac{\lambda^3 h}{2(1+\lambda)} a_{32} - \dfrac{P_0}{(1+\lambda)h^2} \\ a_{22} = -\dfrac{h}{2\lambda(1+\lambda)} a_{31} - \dfrac{\lambda(3+4\lambda)h}{2(1+\lambda)} a_{32} + \dfrac{P_0}{\lambda(1+\lambda)h^2} \end{cases}$$

$$\begin{cases} b_{31} = -\dfrac{2\lambda(1+\lambda)e_{331}e_{332}M_2 V_0}{h^2 Q_a} \\ \quad + \dfrac{2\lambda(1+\lambda)(\lambda e_{331} + e_{332})e_{331}e_{332}M_2 T(\alpha_{12} - \alpha_{11})}{h(d_{311}e_{332} - d_{312}e_{331})Q_a} \\ b_{32} = \dfrac{M_1}{M_2} b_{31} \end{cases} \quad \begin{cases} b_{21} = \dfrac{(4+3\lambda)h}{2(1+\lambda)} b_{31} + \dfrac{\lambda^3 h}{2(1+\lambda)} b_{32} \\ b_{22} = -\dfrac{h}{2\lambda(1+\lambda)} b_{31} - \dfrac{\lambda(3+4\lambda)h}{2(1+\lambda)} b_{32} \end{cases}$$

The expressions of $g_{2i}, g_{1i}, r_{2i}, r_{1i}, r_{0i}, f_{3i}, f_{2i}, f_{1i}, \theta_i, u_{0i}, w_{0i}, J_i, M_i, A_i, Q_a$ refer to Appendix A.

Appendix D

For a piezoelectric heterogeneous bimorph cantilever with constant layer thicknesses, the amendments of tip deflections and electrode charges are expressed as follows, respectively:

$$H_1=\frac{\left[\begin{array}{l}\left(10S_{111}{}^4S_{112}+142S_{111}{}^3S_{112}{}^2+39S_{111}{}^2S_{112}{}^3+16S_{111}S_{112}{}^4+S_{112}{}^5\right)e_{331}{}^2d_{311}{}^2\\-\left(20S_{111}{}^3S_{112}+270S_{111}{}^2S_{112}{}^2+48S_{111}S_{112}{}^3+14S_{112}{}^4\right)e_{331}d_{311}{}^4\\+\left(10S_{111}{}^2S_{112}+128S_{111}S_{112}{}^2+10S_{112}{}^3\right)d_{311}{}^6\end{array}\right]}{\left[\begin{array}{l}\left(S_{111}{}^6+29S_{111}{}^5S_{112}+226S_{111}{}^4S_{112}{}^2+226S_{111}{}^3S_{112}{}^3+29S_{111}{}^2S_{112}{}^4+S_{111}S_{112}{}^5\right)e_{331}{}^3\\-\left(3S_{111}{}^5+72S_{111}{}^4S_{112}+450S_{111}{}^3S_{112}{}^2+408S_{111}{}^2S_{112}{}^3+27S_{111}S_{112}{}^4\right)e_{331}{}^2d_{311}{}^2\\+\left(3S_{111}{}^4+57S_{111}{}^3S_{112}+237S_{111}{}^2S_{112}{}^2+183S_{111}S_{112}{}^3\right)e_{331}d_{311}{}^4\\-\left(S_{111}{}^3+14S_{111}{}^2S_{112}+13S_{111}S_{112}{}^2\right)d_{311}{}^6\end{array}\right]}$$

$$H_2=\frac{\left[\begin{array}{l}\left(13S_{111}{}^2S_{112}+2S_{111}S_{112}{}^2+S_{112}{}^3\right)e_{331}d_{311}{}^2\\-\left(13S_{111}S_{112}+S_{112}{}^2\right)d_{311}{}^4\end{array}\right]}{\left[\begin{array}{l}\left(S_{111}{}^4+15S_{111}{}^3S_{112}+15S_{111}{}^2S_{112}{}^2+S_{111}S_{112}{}^3\right)e_{331}{}^2\\-\left(2S_{111}{}^3+16S_{111}{}^2S_{112}+14S_{111}S_{112}{}^2\right)e_{331}d_{311}{}^2\\+\left(S_{111}{}^2+S_{111}S_{112}\right)d_{311}{}^4\end{array}\right]}$$

$$H_3=\frac{\left(S_{111}S_{112}+S_{112}{}^2\right)d_{311}{}^2}{\left[\begin{array}{l}\left(S_{111}{}^3+14S_{111}{}^2S_{112}+S_{111}S_{112}{}^2\right)e_{331}\\-\left(S_{111}{}^2+13S_{111}S_{112}\right)d_{311}{}^2\end{array}\right]}$$

$$H_4=\frac{\left(S_{112}{}^2-S_{111}{}^2\right)e_{331}d_{311}{}^2+S_{111}d_{311}{}^4}{\left[\begin{array}{l}\left(S_{111}{}^3+14S_{111}{}^2S_{112}+S_{111}S_{112}{}^2\right)e_{331}{}^2\\-\left(2S_{111}{}^2+14S_{111}S_{112}\right)e_{331}d_{311}{}^2+S_{111}d_{311}{}^4\end{array}\right]}$$